PHYSICAL REVIEW A VOLUME 56, NUMBER 4 OCTOBER 1997

Radiative corrections to the electron g-factor in H-like ions

Hans Persson, Sten Salomonson, Per Sunnergren, and Ingvar Lindgren
Department of Physics, Chalmers University of Technology and Göteborg University, S-412 96 Göteborg, Sweden

(Received 8 July 1996; revised manuscript received 29 April 1997)

In view of the current interest of QED in strong fields, a complete set of one-photon radiative corrections to the bound-electron g factor is evaluated for several hydrogenlike ions. The calculations are performed to all orders in the nuclear potential and compared to earlier results, based on the $(Z\alpha)$ expansion, which includes the Schwinger and the Grotch terms. For low Z our all-order result approaches the $(Z\alpha)$ expansion, but for high Z there is a substantial deviation. Furthermore, for high Z our calculations show that the uncertainty due to nuclear structure is small and thus strongly motivate the bound g-factor experiment in progress. [S1050-2947(97)50410-0]

PACS number(s): 31.10.+z, 12.20.Ds, 31.15.Ar, 31.30.Jv

Several different types of experiments on highly charged ions are currently carried out in order to test the validity of quantum electrodynamics (QED) in strong nuclear fields [1–4]. The critical point is to find systems where uncertainties in the nuclear description do not restrict the testing ground. A good candidate, which fulfills the above requirement, is the bound-electron g factor in H-like ions. A Penning-trap experiment is presently being prepared by a Mainz-GSI collaboration to perform such measurements [5]. In the first stage of the experiment, ions in the range $Z=6-20$ will be measured. At a later stage this will be extended to heavier ions up to H-like uranium. The expected relative uncertainty of the measurements is of the order of 10^{-7} and this stimulates theoretical efforts to reach a comparable accuracy.

In Dirac quantum theory the g factor of a free electron is exactly $g=2$. Due to self-interactions with the radiation field, the free electron possesses an anomalous magnetic moment g_e. The investigations of g_e have reached very far, and give at present the outstanding agreement at the level of one part in 10^{11} between theory and experiment [6].

The corrections to the g factor of an atomic electron originate not only from the interactions with the radiation field, but also from the interaction with the nuclear field. Beyond the relativistic Breit correction [7], Grotch and Hegstrom [8–10] did pioneering work in deriving the leading bound radiative correction of order $\alpha(Z\alpha)^2$ and the leading recoil corrections of order $(Z\alpha)^2 m/M$, $\alpha(Z\alpha)^2 m/M$ and $(Z\alpha)^2(m/M)^2$, where m/M is the electron-nucleus mass ratio. However, to obtain accurate theoretical results for heavy ions, one has to go beyond the $(Z\alpha)$ expansion and include the nuclear interaction nonperturbatively.

In this paper we present a calculation of the nonrecoil radiative part [Figs. 1(b)–1(e)] to all orders in $(Z\alpha)$. Selected results for various H-like ions are presented in Tables I and II. As seen from Fig. 2, our self-energy result approaches the Grotch prediction for low Z, but for higher Z there is a substantial deviation. This deviation is due to uncalculated higher-order terms [in $(Z\alpha)$] that are significant for medium and high Z. A similar calculation of the self-energy effects has recently been performed by Blundell, Cheng, and Sapirstein [11]. In the high-Z region we agree well with their calculation, but for low Z our results are slightly larger. Furthermore, for high Z our calculations show that the uncertainty due to nuclear structure is small and thus strongly motivates the bound g-factor experiment being set up in Mainz.

The magnetic dipole moment of a bound electron is conventionally expressed in terms of the g factor as

$$\boldsymbol{\mu}=-g_j\frac{e}{2m}\mathbf{j}=-g_j\mu_B\frac{\mathbf{j}}{\hbar},$$

and the energy in an external magnetic field is given by the scalar product between the dipole moment and the magnetic field. Throughout this paper we will consider a bound electron in a $1s$ state with $m_j=1/2$ ($|a\rangle=|1s^+\rangle$) interacting with a static homogeneous magnetic field aligned in the z direction. The various g-factor corrections can then be extracted from different energy contributions via the relation (in units where $\hbar=\epsilon_0=c=1$)

$$\Delta E=-\langle a|\boldsymbol{\mu}\cdot\mathbf{B}|a\rangle=g_j\mu_B\langle a|j_z|a\rangle B_z=\frac{1}{2}g_j\mu_B B_z. \quad (1)$$

By introducing the minimal coupling in the Dirac equation for an electron in an external homogeneous magnetic field, described by the vector potential $\mathbf{A}=-(\mathbf{r}\times\mathbf{B})/2$, the first-order contribution to the g factor [see Fig. 1(a)] can, in the point nucleus case, be evaluated analytically,

$$g_j^{\text{Breit}}=\frac{2}{\mu_B B_z}\langle a|\boldsymbol{\alpha}\cdot e\mathbf{A}|a\rangle=\frac{2}{3}[1+2\sqrt{1-(Z\alpha)^2}]. \quad (2)$$

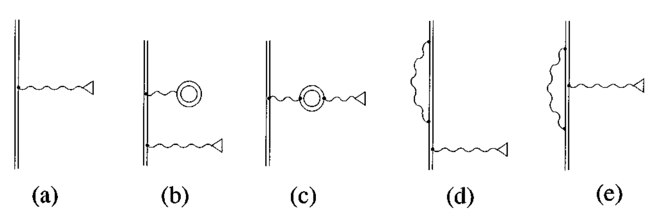

FIG. 1. Feynman diagrams representing the first-order interaction (a) and the one-photon radiative corrections (b)–(e) to the bound-electron g factor. The triangle represents the external magnetic field.

TABLE I. Numerically calculated one-photon QED corrections given in terms of the function $C^{(2)}(Z\alpha)$.

Z	VP	SE	(VP+SE)
1	−0.0	0.500 004 47	0.500 004 47
2	−0.000 000 02	0.500 018 15	0.500 018 13
3	−0.000 000 12	0.500 041 82	0.500 041 70
4	−0.000 000 37	0.500 076 50	0.500 076 14
5	−0.000 000 9	0.500 123 4	0.500 122 5
6	−0.000 001 8	0.500 183 5	0.500 181 7
7	−0.000 003 4	0.500 258 4	0.500 255 0
8	−0.000 005 7	0.500 349 2	0.500 343 5
9	−0.000 009 1	0.500 457 6	0.500 448 5
10	−0.000 013 7	0.500 584 6	0.500 570 9
11	−0.000 019 8	0.500 732 5	0.500 712 7
12	−0.000 027 8	0.500 902 0	0.500 874 2
13	−0.000 038	0.501 095	0.501 057
14	−0.000 051	0.501 313	0.501 262
15	−0.000 067	0.501 556	0.501 489
16	−0.000 086	0.501 829	0.501 743
17	−0.000 109	0.502 130	0.502 021
18	−0.000 133	0.502 463	0.502 330
24	−0.000 408	0.505 194	0.504 786
32	−0.001 244	0.511 23	0.509 99
44	−0.004 306	0.527 19	0.522 88
54	−0.009 738	0.549 01	0.539 27
66	−0.022 28	0.589 41	0.567 14
74	−0.036 49	0.627 95	0.591 46
83	−0.061 4	0.686 3	0.624 9
92	−0.100 6	0.765 5	0.664 9

This expression was first derived by Breit in 1928 [7].

In the following, we will consider the one-photon (second-order) radiative energy corrections that can be related to the g factor by Eq. (1). The Feynman diagrams for these effects can be divided into vacuum polarization [Figs. 1(b) and 1(c)] and self-energy [Figs. 1(d) and 1(e)] parts. The expressions for the one-photon effects can be derived in a formal way, using the S-matrix formalism and the Gell-Mann–Low–Sucher formula [12]

$$\Delta E=\lim_{\eta\to 0}\frac{1}{2}i\eta[3\langle a|S_\eta^{(3)}|a\rangle-3\langle a|S_\eta^{(2)}|a\rangle\langle a|S_\eta^{(1)}|a\rangle]. \tag{3}$$

Here, the second term represents products of disconnected lower-order diagrams. The calculations of the radiative corrections are performed in a way similar to our recently published works [13–15].

The contribution from diagram 1(b), the vacuum polarization wave-function correction, is given by

$$\Delta E_{\mathrm{VP}}^{\mathrm{WF}}=\sum_t \frac{\langle a|V_{\mathrm{VP}}|t\rangle\langle t|\boldsymbol{\alpha}\cdot e\mathbf{A}|a\rangle}{\epsilon_a-\epsilon_t},$$

with $\epsilon_t\neq\epsilon_a$. The singular reference-state contribution $\epsilon_t=\epsilon_a$ is completely cancelled here by the product of lower-order disconnected diagrams in Eq. (3). The vacuum-polarization potential V_{VP} consists of the charge renormalized Uehling part and the remaining many-potential Wichmann-Kroll part [15]. This diagram is readily evaluated using the techniques described in [15].

TABLE II. The total (g_j-2) correction (see text) is collected for some H-like ions. For convenience we have also tabulated the nuclear size correction on the Breit term and the nuclear recoil effect. All values are given in terms of 10^{-6}.

Z	R_{rms} (fm)	Nuc. size	Nuc. recoil	Total
1		0.0	0.029	2 283.853
2		0.0	0.029	2 177.406
3		0.0	0.037	1 999.988
4		0.0	0.051	1 751.573
5		0.0	0.066	1 432.121
6		0.0	0.087	1 041.590
7	2.540(20)	0.0	0.10	579.91
8	2.737(8)	0.0	0.12	47.02
9	2.90(2)	0.0	0.12	−557.17
10	2.992(8)	0.0	0.14	−1 232.72
11	2.94(6)	0.01	0.15	−1 979.78
12	3.08(5)	0.01	0.17	−2 798.42
13	3.035(2)	0.01	0.18	−3 688.80
14	3.086(18)	0.02	0.20	−4 651.04
15	3.191(5)	0.03	0.21	−5 685.31
16	3.230(5)	0.04	0.23	−6 791.75
17	3.388(17)	0.05	0.24	−7 970.55
18	3.423(14)	0.07	0.23	−9 221.91
24	3.643(3)	0.27	0.3	−18 265.6
32	4.088(8)	1.24	0.4	−34 495.1
44	4.480(22)	6.92(6)	0.6	−68 165.8
54	4.782(2)	23.4(2)	0.6	−105 359.5
66	5.211(26)	90.9(8)	0.8	−162 107.5
74	5.374(22)	205.6(14)	0.9	−208 166.2
83	5.519(4)	500.0(6)	1.0	−268 988.6
92	5.860(2)	1 274.1(6)	1.0	−340 793.4

Diagram 1(c) can also be divided into a Uehling part and a Wichmann-Kroll part. In momentum space, the $\mathbf{r}$ operator in the vector potential transforms into the gradient of a δ function

$$\mathbf{r}\to i\nabla_{\mathbf{k}}\delta(\mathbf{k}). \tag{4}$$

The Uehling contribution of diagram 1(c) is thus proportional to the integral

$$\int\frac{d^3\mathbf{k}}{(2\pi)^3}\Psi_a^\dagger(\mathbf{k})\{\nabla_{\mathbf{k}}\delta(\mathbf{k})\}\Pi^{\mathrm{ren}}(\mathbf{k}^2)\Psi_a(\mathbf{k}),$$

where $\Pi^{\mathrm{ren}}(\mathbf{k}^2)$ is the renormalized free-electron polarization function. By means of partial integration and utilizing that the polarization function behaves as $\mathbf{k}^2$ for small momenta, this contribution can be seen to vanish. The Wichmann-Kroll part, however, is nonvanishing and has been evaluated in the same way as in previous work [13].

More care has to be taken when considering the self-energy contributions. The nondegenerate part of diagram 1(d), the self-energy wave-function correction, can be written as

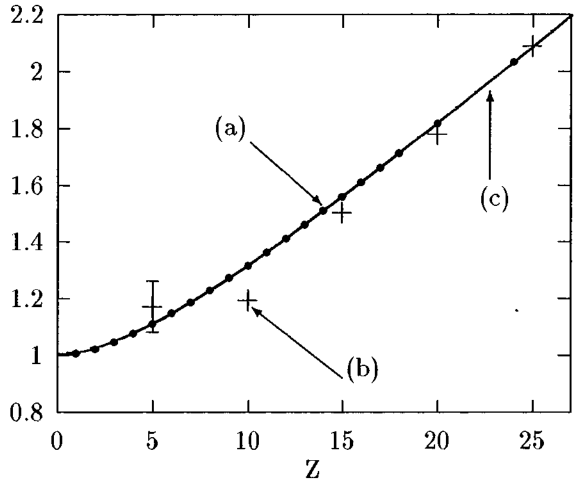

FIG. 2. The one-photon self-energy contributions after subtracting the Schwinger term and dividing with the Grotch term. The dots (a) show our numerical values and the line (c) is a fit to these values. As a comparison the values of Blundell *et al.*, crosses (b), are also shown.

$$\Delta E_{\mathrm{SE}}^{\mathrm{WF}}=\sum_t \frac{\langle a|(\Sigma-\delta m)|t\rangle\langle t|\boldsymbol{\alpha}\cdot e\mathbf{A}|a\rangle}{\epsilon_a-\epsilon_t},$$

with $\epsilon_t \neq \epsilon_a$. Here Σ denotes the unrenormalized bound self-energy operator and δm the mass counter term. The divergences in this expression are isolated and subtracted by means of a potential expansion of the self-energy operator into a free self-energy operator, a one-potential term, and a finite many-potential part. The many-potential part is treated in coordinate space in a similar way as in previous works [13,14,16,17]. The divergent zero- and one-potential terms are grouped together with the mass counter term, and by the use of dimensional regularization the finite parts can be extracted and calculated in momentum space [18].

The degenerate part of diagram 1(d) is singular and one has to subtract products of disconnected lower-order diagrams to cancel the reference-state singularity [see Eq. (3)]. After the subtraction, the remainder is given by

$$\Delta E_{\mathrm{SE}}^{\mathrm{ref}}=\langle a|\boldsymbol{\alpha}\cdot e\mathbf{A}|a\rangle\times\left\langle a\left|\left(\frac{\partial}{\partial\epsilon}\Sigma(\epsilon)\right)_{\epsilon=\epsilon_a}\right|a\right\rangle. \tag{5}$$

The contribution due to the vertex diagram 1e is

$$\Delta E_{\mathrm{SE}}^{\mathrm{vert}}=\langle a|\boldsymbol{\Lambda}\cdot e\mathbf{A}|a\rangle, \tag{6}$$

where $\boldsymbol{\Lambda}$ is the vector vertex function [18]. The two expressions in Eqs. (5) and (6) are both infrared and ultraviolet divergent, but the divergences cancel between the two terms. To formulate an unambiguous regularization, we expand the intermediate bound electron propagators in Eqs. (5) and (6) into free-electron propagators interacting zero, one, or several times with the nuclear potential. After separating out and cancelling the infrared divergences [13], the one-potential and many-potential terms are finite and can readily be calculated in coordinate space using basis-set procedures [19]. The zero-potential terms can be grouped together, and by the use of dimensional regularization the ultraviolet divergences can be identified and cancelled. The finite remainder was evaluated in momentum space.

A difference from earlier elaborations of a similar type [13,14] is that the momentum space expression involves the gradient of a δ function [see Eq. (4)]. We have chosen to represent this highly singular function numerically by introducing a Gaussian cutoff function in coordinate space that yields the gradient of a Gaussian δ function in the Fourier transform

$$\mathbf{r}e^{-(\rho r/2)^2}\rightarrow i\nabla_{\mathbf{k}}\frac{1}{\pi^{3/2}\rho^3}e^{-(k/\rho)^2}=-i\mathbf{k}\frac{2}{\pi^{3/2}\rho^5}e^{-(k/\rho)^2}.$$

Eventually, the limit $\rho\rightarrow 0$ should be taken, but in practice it is enough to have a small finite value of ρ so that the introduced inhomogeneity in the magnetic field is negligible over the extension of the ion.

To discuss the results, it is convenient to expand the g factor into zero-, one-, etc. photon contributions. Specifically, for an electron bound to an infinitely heavy point nucleus, the expansion is given by (the power of α/π indicates the number of virtual photons)

$$g_j=2\left\{\frac{1}{3}[1+2\sqrt{1-(Z\alpha)^2}]+\frac{\alpha}{\pi}\left(\frac{1}{2}+\frac{(Z\alpha)^2}{12}+\cdots\right)+\left(\frac{\alpha}{\pi}\right)^2(A^{(4)}+\cdots)+\left(\frac{\alpha}{\pi}\right)^3(A^{(6)}+\cdots)+\cdots\right\}, \tag{7}$$

where $A^{(4)}=-0.328\,478\ldots$ and $A^{(6)}=1.18\ldots$ are the known free-electron contributions [6]. Focus now on the one-photon contributions in Eq. (7) described by the function $C^{(2)}(Z\alpha)=1/2+(Z\alpha)^2/12+\cdots$, where the first term is the Schwinger correction and $(Z\alpha)^2/12$ is the Grotch term [9]. For low Z, 1/2 strongly dominates (for $Z=1$ by five orders of magnitude). Thus, to achieve the QED corrections beyond the Schwinger term, one needs a very high numerical accuracy in the calculations for low Z. To reach this accuracy for $Z=1$ in the one-potential vertex part, one has to go well beyond 100 partial waves. The results are given in Table I and the self-energy contributions beyond Schwinger divided by Grotch are displayed in Fig. 2. For the self-energy terms we agree well with the results of [11] except for $Z=10$, 15, and 20, where there is minor deviation.

From a $(Z\alpha)$ expansion consideration, beyond the Schwinger and Grotch term, one would expect terms of order $\alpha(Z\alpha)^4$ [20]. For $Z\leqslant 30$ we have performed different fittings of our numerical values, beyond the Schwinger correction, to formulas of the type

$$A\alpha(Z\alpha)^2+\alpha(Z\alpha)^4[B+C\ln(Z\alpha)+D(Z\alpha)]$$

and obtained the Grotch coefficient A with an accuracy better than 1%. Since the displayed ratio in Fig. 2 becomes very sensitive for $Z=1$ we get a safer prediction by using different fittings of the results from higher Z. Our fitted result of this ratio for $Z=1$ is 1.007(2), where the uncertainty comes from excluding the log term in the fitting function. This value is also consistent with our numerical value for $Z=1$ given in Table I.

To make a comparison with experiment one has to include the effects of nuclear recoil, finite nuclear size, and QED corrections from diagrams involving two and more virtual photons. Additionally, for very high Z also effects from nuclear polarization might come in at the 10^{-7} level.

The nuclear recoil correction can be obtained from the formulas derived by Grotch and Hegstrom [10], and is to the demanded accuracy given by the leading term $g_j^{\text{recoil}}=(Z\alpha)^2 m/M$. For high Z this can only be considered as a reliable order-of-magnitude estimation [21]. However, in this region this is sufficient since the recoil effect is small compared to the bound-state QED corrections.

Furthermore, a careful investigation of the nuclear size effect on the dominating first-order contribution has been performed. A two-parameter Fermi distribution was used for the nuclear description. For all nuclei the default a-parameter $a=0.524$ was used, except for uranium where $a=0.6023$ was taken to simulate a deformed Fermi model [22]. The uncertainty assigned to the nuclear-size effect in Table II corresponds to the experimental uncertainty in the R_{rms} values [23].

Concerning the QED effects involving two and more virtual photons, the free-electron part is significant. The corresponding bound-state corrections, which are still uncalculated, should be a factor (α/π) smaller than the calculated one-photon bound-state corrections.

In the last column of Table II we have added all different contributions, i.e., the one-photon bound-state correction, the nuclear-size effect (column 3), the nuclear recoil (column 4), the (g_j-2) from the Breit term [Eq. (2)], and the free-electron (g_e-2) value.

The uncertainty in the theoretical values are small compared to the bound-state QED effects for all Z. With an anticipated experimental uncertainty of 10^{-7}, this implies that the bound-state g-factor measurements will constitute a good test of bound-state QED for all $Z\geqslant 10$.

We wish to express our gratitude to K. Pachucki, W. Quint, various members of the Mainz group, E. Lindroth, G. Soff, S. Schneider, the atomic physics group at GSI, and B. N. Taylor for stimulating discussions. Also we want to thank J. Sapirstein, K. T. Cheng, and S. A. Blundell for providing us their results before publication. This work has been supported by the Swedish NFR and the von Humboldt Stiftung.

[1] J. Schweppe *et al.*, Phys. Rev. Lett. **66**, 1434 (1991).
[2] I. Klaft *et al.*, Phys. Rev. Lett. **73**, 2425 (1994).
[3] H. F. Beyer *et al.*, Z. Phys. D **35**, 169 (1995).
[4] R. E. Marrs, S. R. Elliott, and Th. Stöhlker, Phys. Rev. A **52**, 3577 (1995).
[5] K. Hermanspahn, W. Quint, S. Stahl, M. Tönges, G. Bollen, H.-J. Kluge, R. Ley, R. Mann, and G. Werth, Acta Phys. Pol. B **27**, 357 (1996).
[6] T. Kinoshita, Phys. Rev. Lett. **75**, 4728 (1995).
[7] G. Breit, Nature (London) **122**, 649 (1928).
[8] R. A. Hegstrom, Phys. Rev. **184**, 17 (1969).
[9] H. Grotch, Phys. Rev. Lett. **24**, 39 (1970).
[10] H. Grotch and R. A. Hegstrom, Phys. Rev. A **4**, 59 (1971).
[11] S. A. Blundell, K. T. Cheng, and J. Sapirstein, Phys. Rev. A **55**, 1857 (1997).
[12] M. Gell-Mann and F. Low, Phys. Rev. **84**, 350 (1951); J. Sucher, *ibid.* **107**, 1448 (1957).
[13] H. Persson, S. Salomonson, P. Sunnergren, and I. Lindgren, Phys. Rev. Lett. **76**, 204 (1996).
[14] H. Persson, S. M. Schneider, W. Greiner, G. Soff, and I. Lindgren, Phys. Rev. Lett. **76**, 1433 (1996).
[15] H. Persson, I. Lindgren, S. Salomonson, and P. Sunnergren, Phys. Rev. A **48**, 2772 (1993).
[16] S. A. Blundell and N. J. Snyderman, Phys. Rev. A **44**, R1427 (1991).
[17] K. T. Cheng, W. R. Johnson, and J. Sapirstein, Phys. Rev. A **47**, 1817 (1993).
[18] N. J. Snyderman Ann. Phys. (N.Y.) **211**, 43 (1991).
[19] S. Salomonson and P. Öster Phys. Rev. A **40**, 5548 (1989); **40**, 5559 (1989).
[20] K. Pachucki (private communication).
[21] A. N. Artemyev, V. M. Shabaev, and V. A. Yerokhin, Phys. Rev. A **52**, 1884 (1995).
[22] A. Ynnerman, J. James, I. Lindgren, H. Persson, and S. Salomonson, Phys. Rev. A **50**, 4671 (1994).
[23] H. De Vries, C. W. Jager, and C. De Vries, At. Data Nucl. Data Tables **36**, 495 (1987); E. G. Nadjakov, K. P. Marinova, and Yu. P. Gangrsky, *ibid.* **56**, 133 (1994); G. Fricke *et al.*, *ibid.* **60**, 177 (1995).